GSR_2
School of Mathematical and Geospatial Sciences, RMIT University
Monday 10 to Wednesday 12 December 2012

GEOMETRIC ACCURACY EVALUATION OF THEOS IMAGERY

[a]Chunsun Zhang, [b]Clive S. Fraser

[a]School of Mathematical and Geospatial Sciences, RMIT University
Melbourne VIC 3001, Australia
Phone: +61 3 9925 2424, Fax: +61 3 9925 2454
Email: chunsun.zhang@rmit.edu.au

[b]Cooperative Research Centre for Spatial Information
Level 5, 204 Lygon Street, Carlton Vic 3053, Australia
Phone: +61 3 8344 9182, Fax: +61 3 9349 5185
Email: c.fraser@unimelb.edu.au

KEY WORDS: Pushbroom sensor, high resolution satellite imagery, georeferencing, accuracy evaluation

ABSTRACT:
This paper presents the georeferencing performance of the imagery from the Thailand Earth Observation System satellite (THEOS) using a generic sensor model developed at the Cooperative Research Centre for Spatial Information (CRCSI), Australia. THEOS provides 2m resolution imagery worldwide together with camera parameters, orbit and attitude data. An assessment of the planimetric accuracy of georeferencing from THEOS imagery, both for single scenes and image strips, has been carried out within a 25 x 110km test field area in Australia, in which a dense array of GPS-surveyed points were established. The test imagery comprised a strip of five images collected within the same orbit. The generic sensor model and integration of the THEOS orientation parameters into the model are first described, along with a brief account of the estimation of camera interior orientation parameters and the concept of strip adjustment. Further investigation reveals presence of errors in the satellite line-of-sight data, possibly caused by mis-alignment of detectors in CCD array, yielding imprecise interior orientation of the sensor. Such errors can be effectively accounted for through modelling via a cubic polynomial, leading to sub-pixel georeferencing accuracy. The test data and experimental procedure are then discussed and the results of the georeferencing of both single images and the 5-image strip as a single entity, via a strip adjustment approach, are presented. The results demonstrate that sub-pixel 2D geopositioning accuracy can be achieved with single THEOS images and within strips of up to three images with as few as six ground control points (GCPs) to effect an orbit adjustment, whereas accuracy decreases to near the 2-pixel level over a strip length of five images.

1. INTRODUCTION

High-resolution satellite imagery (HRSI) with a spatial resolution of 2.5m or better is becoming increasingly accessible to the mapping and GIS community. The Thailand Earth Observation System satellite (THEOS), as a relatively new HRSI system, provides imagery at a theoretical spatial resolution of 2 m over a swath width of 24 km. THEOS imagery offers the potential for orthoimage generation and metric information extraction in support of medium-scale mapping and GIS applications. To exploit full metric quality of optical satellite imagery and precise georeferencing, a number of sensor orientation models have been developed over the past three decades. These have ranged from empirical models, through to camera replacement models such as the now popular rational function model (Fraser and Hanley, 2003), and to rigorous parametric formulations which model the physical image-to-object space transformation (Kratky, 1989; Westin, 1990; Chen and Lee, 1993; Dowman and Michalis, 2003; Poli, 2005; Kim and Dowman, 2006). Generic models are an effective solution that have been adopted for many satellite imaging systems (Poli, 2005; Weser at al., 2008; Fraser at al., 2007; Michalis and Dowman, 2008). The models take full account of the physical imaging process and adopt time dependant satellite orbit models and interior

* Review Paper – accepted after double-blind review.
ISBN: 978-0-9872527-1-5
Melbourne: Geospatial Sciences, RMIT 2012

orientation (IO) information provided by the satellite imagery vendors. Moreover, given the increasing number of HRSI satellites being deployed, the attraction of a generic sensor orientation model suited to a wide range of satellite imagery becomes compelling. The advantage of the physical model is that it is flexible in that it can be readily adapted to most HRSI vendor-specific definitions for sensor orientation (Weser at al., 2008; Michalis and Dowman, 2008; Rottensteiner et al., 2009). The compensation of systematic errors inherent in vendor-supplied orientation data is achieved through a least-squares sensor orientation adjustment, which incorporates additional parameters for bias compensation and employs a modest number of ground control points (GCPs).

This paper reports on an investigation of the application of the generic sensor orientation model to precise georeferencing of THEOS satellite imagery. In the following section, the generic sensor orientation model is briefly reviewed and the handling of THEOS metadata within the model is presented. This is followed by a discussion of a correction model that was found to compensate apparent errors in the provided sensor IO parameters. Afterwards, the test site and test data are described, followed by a discussion of the conduct and results of the experimental evaluation of georeferencing for a 5-scene THEOS data set covering a 100km x 25km test field running north from the city of Melbourne.

2. GENERIC SENSOR ORIENTATION MODEL

2.1 Overview

The generic sensor model adopted, which was developed within the CRCSI, is a combination of physical and empirical parameters, the latter being the cubic splines used to model the satellite trajectory and attitude, and the polynomial used to model errors in the interior orientation. A feature of this sensor model is that vendor-specific definitions of transformation parameters are mapped to the general model. Thus, it is applicable to a variety of pushbroom scanners, and has previously been successfully applied to a number of current high-resolution satellite imaging systems, including GeoEye-1, WorldView-1 and -2, IKONOS, QuickBird, SPOT5, Cartosat-1 and ALOS PRISM (Weser at al., 2008; Fraser at al., 2007; Rottensteiner et al., 2009). Whereas full details of the model can be found in Weser et al. (2008), a short summary will be presented here. Figure 1 shows the coordinate systems in the model.

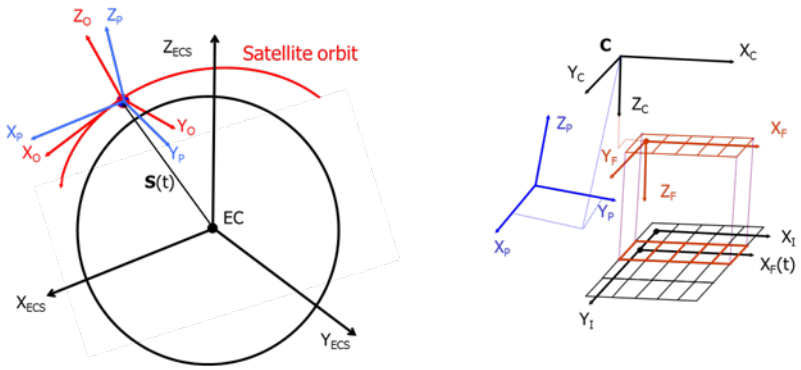

Figure 1. (Left) Object (X_{ECS}, Y_{ECS}, Z_{ECS}), orbital (X_O, Y_O, Z_O) and platform (X_P, Y_P, Z_P) coordinate systems. (Right) Camera (X_C, Y_C, Z_C), Detector (X_F, Y_F, C_F) and image file (X_I, Y_I) coordinate systems.

* Review Paper – accepted after double-blind review.
ISBN: 978-0-9872527-1-5
Melbourne: Geospatial Sciences, RMIT 2012

The generic sensor model for pushbroom scanners, which relates an object point P_{ECS} in an earth-centered object coordinate system to its projected point $P_I = (x_I, y_I, 0)^T$ in the image plane coordinate system, is expressed as

$$P_{ECS} = S(t) + R_O \cdot R_P(t) \cdot [C_M + \lambda \cdot R_M \cdot (p_F - c_F + \delta x)] \quad (1)$$

Within each image line, there is a central projection between the image point $P_F = (x_I, 0, 0)^T$ in the detector coordinate system and the corresponding point P_{ECS}, with the y_I image coordinate being a function of time $t = t_0 + \Delta t \cdot y_I$, t_0 being the acquisition time of the first image line. In Eq. 1, the vector c_F is the position of the projection centre in the detector coordinate system, and δx formally describes the image biases (eg refraction and residual systematic errors). The rotation matrix R_M and the translation C_M describe the rigid motion of the camera with respect to the satellite platform. $S(t)$ models the time-dependent orbit path. The time-constant rotation matrix R_O rotates from the earth-centred coordinate system to a system defined at the scene centre tangent to the orbit path. The time-dependent rotation matrix $R_P(t)$ rotates from the defined orbit system to the satellite platform system, parameterised by three time-dependent rotation angles: roll, pitch, and yaw. The components of the orbit path and the time-dependant rotation angles are in turn modelled by cubic spline functions. The coefficients of the spline function are initialised from the orbit and attitude data recorded on board the satellite. The generic sensor orientation model can also treat a continuous strip of images recorded in the same orbit. Under this approach, the orbit path and attitude data for each separate scene of a strip are merged to produce a single, continuous set of orbit and attitude observations, such that the entire strip of images can be treated as a single image, even though the separate scenes are not merged per se (Rottensteiner et al., 2009; Fraser and Ravanbakhsh, 2010). The merging of orbit data results in a considerable reduction in the number of unknown orientation parameters, and thus also in the number of required GCPs, which can then be as few as two at each end of the strip.

2.2 Incorporation of THEOS Sensor Model

Based on the analysis of the metadata provided in GISTDA (2010), the relationship between an object point P_{ECS} and p_F for THEOS can be expressed as

$$P_{ECS} = S(t) + R_{IF}(t) \cdot R_T{}^T(t) \cdot P_P \quad (2)$$

where P_P denotes the platform coordinates, $R_T(t)$ the rotation between the satellite platform system and the earth-centred inertial (ECI) system at time *t*, and $R_{IF}(t)$ the rotation from the ECI system to the earth-centred fixed (ECF) system. $R_{IF}(t)$ comprises four rotation terms, namely precession, nutation, earth rotation of Greenwich apparent sidereal time and polar motion (Xu, 2007). A comparison of Eq. 2 with the generic sensor model of Eq. 1 yields $R_O \cdot R_P(t) = R_{IF}(t) \cdot R_T{}^T(t)$, which results in an expression for the time-dependent rotation $R_P(t)$ from the orbit system to the platform system:

$$R_P(t) = R_O{}^T \cdot R_{IF}(t) \cdot R_T{}^T(t) \quad (3)$$

The interior orientation (IO) parameters can be estimated from the viewing angles ψ_x and ψ_y of each pixel in the line-of-sight reference frame R_{LOS} (see Fig. 2). These values are provided in the metadata in the form of cubic polynomials, and the position of each pixel in R_{LOS} is expressed as

$$P_{LOS} = [\tan(\psi_y), -\tan(\psi_x), 1]^T \quad (4)$$

There is a small rotation between R_{LOS} and the platform coordinate system R_{SAT}. This is given in the form of three bias angles: roll, pitch, and yaw, which can be used to compute the bias rotation matrix R_{bias} such that

* Review Paper – accepted after double-blind review.
ISBN: 978-0-9872527-1-5
Melbourne: Geospatial Sciences, RMIT 2012

$$P_P = R_{bias} \cdot P_{LOS} \tag{5}$$

The relationship between P_{LOS} and the detector coordinate p_F can be expressed by

$$P_{LOS} = \lambda R_C \left(p_F - c_F \right) \tag{6}$$

A comparison of Eqs. 1 and 2, with reference to Eqs. 5 and 6, reveals that

$$C_M = 0 \tag{7}$$

$$R_M = R_{bias} \cdot R_C \tag{8}$$

Cubic splines of third order are employed to model the time-dependent satellite orbit $S(t)$ and the rotation angles forming $R_P(t)$. Within the subsequent least-squares orientation adjustment, the parameters comprise the polynomial coefficients of the spline functions, the three coordinate components of the orbit $S(t)$, the three rotation angles of $R_P(t)$ and the positions P_{ECS} of the object points. Bias-correction parameters for orbit and attitude data can also be included. The observations comprise the framelet coordinates p_F, and the GCPs are also treated as direct observations.

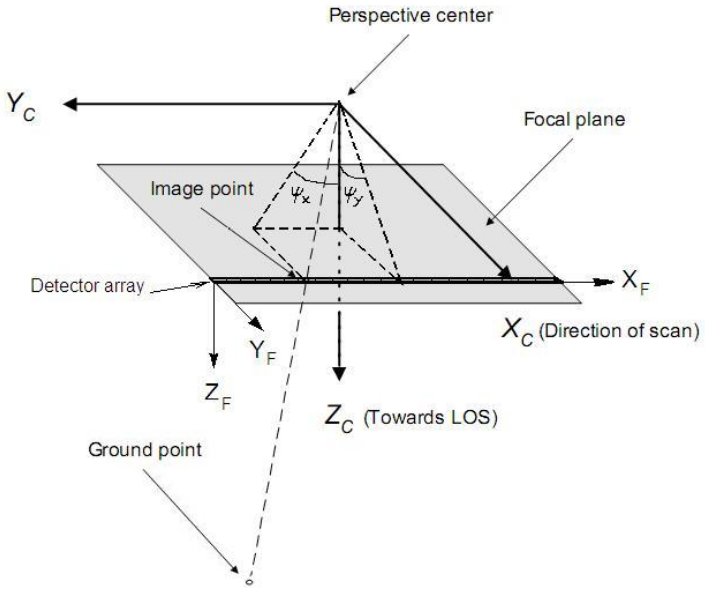

Figure 2. Line-of-sight reference system (X_C,Y_C,Z_C), detector coordinate system (X_F,Y_F,Z_F) and instrument view angles (ψ_x,ψ_y).

Modelling and Correction of Interior Orientation

The IO parameters and the detector mounting rotation angles of THEOS can be computed by spatial resection based on Eq. 7 using the instrument view angles provided in the metadata. The relationship between each pixel *i* in the linear array and the view angles is given as

$$\begin{pmatrix} \tan\psi_y \\ -\tan\psi_x \\ 1 \end{pmatrix} = \lambda \cdot \begin{pmatrix} r_{11} & r_{12} & r_{13} \\ r_{21} & r_{22} & r_{23} \\ r_{31} & r_{32} & r_{33} \end{pmatrix} \cdot \begin{pmatrix} i - x_0 \\ 0 - y_0 \\ 0 - z_0 \end{pmatrix} \tag{9}$$

Here, r_{ij} is the element of the rotation matrix R_C from the three rotation angles roll, pitch and yaw, and x_0, y_0 and z_0 are the offset parameters of the perspective centre. Therefore, the IO parameters and the rotation angles forming matrix R_C can be estimated by an iterative least squares adjustment. As all the points lie on a straight line, the rotation angle about the X_F axis, which cannot be determined, is assigned a constant value

* Review Paper – accepted after double-blind review.
ISBN: 978-0-9872527-1-5
Melbourne: Geospatial Sciences, RMIT 2012

of zero. Because of the high correlation between the rotation angles and the offsets, e.g. roll is highly correlated with x_0 and pitch with y_0, the normal equation system of the least-squares adjustment would be ill-conditioned, leading to the potential recovery of erroneous values for the parameters. Weighted constraints can be applied to alleviate this problem, for example the angle pitch can be constrained to a near-zero value.

The quality of IO estimation relies on the precision of the view angles modelled by cubic polynomials. Errors in these angles result in large observational residuals and potentially poor quality IO parameters, which in turn degrade the geometric potential of THEOS imagery. It was found in the reported investigation that errors in IO can result in a deterioration of up to 2 pixels in 2D georeferencing accuracy in the cross track direction, as will be discussed later in the paper.
Self-calibration is an efficient technique for the modelling and elimination of the systematic errors of satellite sensors (Kocaman and Gruen, 2008). However, self-calibration approaches require a significant amount of well-distributed GCPs. Moreover, the results are not always stable due to the correlation between the model parameters. Full set of radial and tangential distortion parameters are difficult to address, and the appropriate parameters have to be selected based on the analysis of their correlations and quality (Radhadevi et al., 2011).

In this investigation, compensation of errors in IO parameters are achieved via polynomial correction functions:

$$\delta x = a_0 + a_1 x + a_2 x^2 + a_3 x^3 + \cdots$$
$$\delta y = b_0 + b_1 x + b_2 x^2 + b_3 x^3 + \cdots \quad (10)$$

where δx and δy denote image space coordinate residuals, x is the sample coordinate along the detector array, and a_i and b_i are the model coefficients. The order of the polynomials depends upon the character of the distribution of residuals. As will be illustrated in Section 4, the distribution of IO residuals found for THEOS imagery indicated a behaviour conducive to modelling via a cubic polynomial function, and this modelling has proved necessary if sub-pixel georeferencing accuracy is to be achieved.

3. EXPERIMENTAL TEST DATA

The test data, supplied by GISTDA, comprised a strip of five mono THEOS panchromatic images over an area north of Melbourne, Australia. The sequence of imagery was recorded within a single orbit on 21 July, 2009. Each scene covered an area of about 23.0 km wide x 24.6 km long, and the total strip length was 107km (there was an approximate 13% overlap between the successive scenes). Within the metadata, the number of orbit observation points outside the image strip was restricted to one before the first scene, whereas the final observation was prior to the last image line of the strip. Generally, for optimal application of the generic sensor model, orbit observations need to not only span the full strip, but also extend into the scenes immediately before the first image and after the last. As will be seen in the analysis of the results, the lack of such orbit data compromised the accuracy of the orbit adjustment and georeferencing to an extent, especially when the strip was treated as a single entity, i.e. as one long image.

The THEOS test field contained 82 GPS-surveyed points with an accuracy of better than 0.2m, i.e. equivalent to better than 0.1 pixel in image space. Due to inadequate orbit observations at the two ends of the strip, some eight points at the strip extremities were omitted from the analysis, thus leaving 74 points. The GCPs were mainly road roundabouts or road intersections that were clearly distinguishable in the images. They were measured to an estimated accuracy of around 0.3-0.5 pixels. The strip layout and GCP locations are indicated in Figure 3.

* Review Paper – accepted after double-blind review.
ISBN: 978-0-9872527-1-5
Melbourne: Geospatial Sciences, RMIT 2012

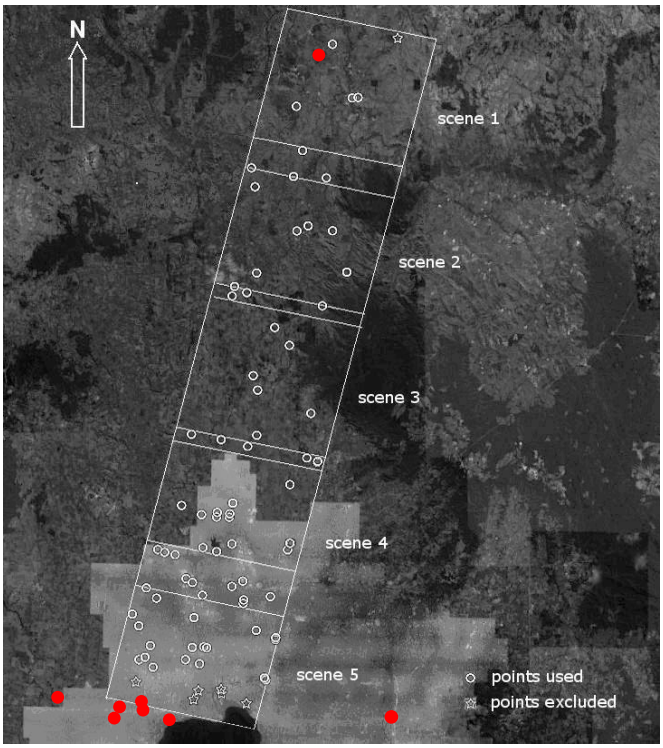

Figure 3. THEOS 5-image strip and distribution of GCPs.

4. RESULTS AND DISCUSSION

4.1 Estimation of Interior Orientation Parameters

An initial determination of the IO parameters and camera mounting rotations was first made from the viewing angles computed according to the provided cubic polynomial coefficients. The values obtained are listed in Table 1.

Table 1. Computed interior orientation parameters of THEOS imagery.

	c_F			R_C		
	x_0 (pixel)	y_0 (pixel)	z_0 (pixel)	*roll* (degrees)	*pitch* (degrees)	*yaw* (degrees)
Value	6000.8	0.0	-446884.7	0.0000	+0.0000	-90.0013
Std. Error	1.3	0.2	18.9	fixed	0.0002	0.0024

The estimated value of x_0 shown in Table 1 indicates that the perspective centre lay within a pixel of the centre of the 12,000-pixel linear array, and the view angles provided in the metadata were symmetric about the array centre. It is noteworthy that whereas the residuals in the *y* coordinate (flight direction) were generally of a magnitude of less than 0.5 pixels, they grew to 1 pixel at the end regions of the detector. The residuals in *x*, on the other hand, reached 7 pixels at the two ends of the detector as illustrated in Figure 4. The large residual values encountered, which displayed a very systematic distribution, suggested either the presence of errors in the provided look angles or imprecise detector alignment within the CCD array, the former being a more plausible assumption. It can be seen from Figure 4 that the residuals are distributed symmetrically about the centre of the linear array. Whereas *y*-residuals show a parabolic distribution, the distribution for *x*-residuals is more complex, with more than 90% of values being beyond 1 pixel.

* Review Paper – accepted after double-blind review.
ISBN: 978-0-9872527-1-5
Melbourne: Geospatial Sciences, RMIT 2012

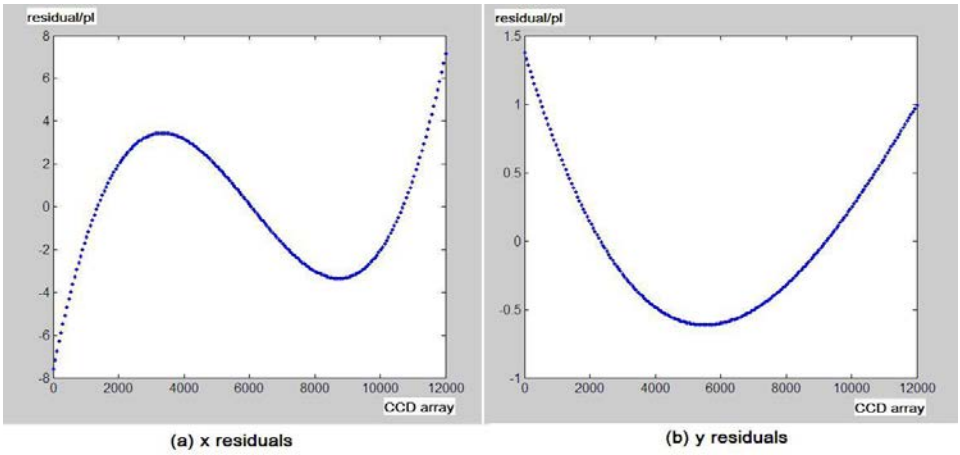

Figure 4. Residuals of IO estimation for THEOS imagery.

In order to examine the impact on accuracy of the presence or absence of the applied polynomial correction function for IO, two sets of sensor orientation adjustments were carried out, both utilizing all GCPs as error free observations. The results for the two cases of with and without image coordinate correction are listed for each scene in Table 2.

Table 2. Accuracies obtained with/without image correction for IO.

Scene ID	Number of GCPs	Without image correction (pixel)		With image correction (pixel)	
		RMSEx	RMSEy	RMSEx	RMSEy
Scene 1	8	2.72	0.36	0.21	0.36
Scene 2	13	2.33	0.31	0.26	0.33
Scene 3	16	1.89	0.42	0.39	0.28
Scene 4	32	1.99	0.49	0.35	0.34
Scene 5	29	2.83	0.48	0.30	0.27

It can be seen that when the image coordinates are directly used without correction, the RMSE in *x* (detector axis) exceeds 2 pixels, whereas with corrected image coordinates, the corresponding RMSE value reduces to under 0.4 pixels in all scenes. This is consistent with the estimated image coordinate measurement accuracy, and with the RMSE value in the y coordinate where there was no significant systematic error signal. Subsequent sensor orientation adjustments reported here all employed the proposed IO correction function.

4.2 Sensor Orientation and 2D Georeferencing

Due to the single image THEOS coverage, only 2D accuracy analysis was possible in object space. A complete 3D sensor orientation could be performed using different GCP configurations, but then checkpoint accuracy could only be quantified in image space via a back projection of 3D checkpoint coordinates into image space using the adjusted orientation parameters, or in object space in 2D using forward projection to an established height value. A direct georeferencing was initially performed, using the THEOS geometric model, Eq. 2, generated from the metadata. No GCPs were employed. Essentially this process afforded an evaluation of the magnitude of biases within the direct georeferencing process. The resulting image point discrepancies (i.e. measured versus back-projected) averaged around 8 pixels in *x* and 29 pixels in *y*. This highlighted the fact that GCPs were going to be essential if absolute georeferencing to 1-pixel level was to be achieved.

* Review Paper – accepted after double-blind review.
ISBN: 978-0-9872527-1-5
Melbourne: Geospatial Sciences, RMIT 2012

The generic model was then applied, with GCPs being used for absolute orientation and orbit/attitude bias correction. Adjustments were performed for both single images and strips comprising 2 – 5 images, with different numbers of GCPs, ranging from all points to as few 6 points for the entire 5-image strip. Two cases will be considered here: 1) The use of all ground points as GCPs, and 2) the use of 6 GCPs, with the remainder being considered as checkpoints. The first case indicates internal accuracy and thus affords an insight into the fidelity of the sensor orientation model. The second case affords an assessment of planimetric accuracy in georeferencing from a modest number of GCPs.

In Case 1, the GCPs were not tightly constrained within the adjustment, but instead assigned a priori standard error of 3m (equivalent to 1.5 pixels). The adjustment could thus be thought of as a relative orientation which best fits the full array of GCPs, without the imposition of shape constraints. It is then possible to infer the accuracy of the sensor orientation process from the RMS discrepancies of adjusted planimetric positions of GCPs in object space. Three different bias-correction parameter sets were employed in the adjustments, namely a shift correction of the orbit path only (termed Model P), three attitude correction parameters (Model A), and 6 correction terms for orbit and attitude (Model PA). However, the 3-parameter attitude correction Model A produced the same results as the 6-parameter Model PA and so only two columns of RMSE values for planimetric coordinates are shown in Table 3. From the table it can be seen that attitude correction Model A is more effective than the orbit shift model, especially in the along-track direction. This indicates an incomplete error compensation in the *pitch* angle data (recall the 29 pixel error in the direct georeferencing).

Table 3. Internal planimetric georeferencing accuracy expressed via RMS discrepancies at GCPs.

Number of merged scenes	Scene index	Number of GCPs (sigma=3 m)	RMSE, Model P		RMSE, Models A & PA	
			Easting/m	Northing/m	Easting/m	Northing/m
1 scene	1	8	0.71	2.72	0.45	0.80
	2	13	0.60	2.18	0.56	0.64
	3	16	0.48	2.08	0.55	0.51
	4	32	0.60	1.31	0.62	0.72
	5	29	0.48	1.09	0.50	0.54
2 scenes	1,2	17	1.08	3.13	0.92	1.80
	2,3	26	0.60	2.01	0.61	0.69
	3,4	42	0.64	1.50	0.68	0.90
	4,5	50	0.57	1.32	0.60	0.80
3 scenes	1,2,3	30	1.00	3.23	0.93	2.33
	2,3,4	52	1.08	1.77	1.07	1.08
	3,4,5	60	0.63	1.91	0.66	1.64
4 scenes	1,2,3,4	56	1.39	2.70	1.30	2.16
	2,3,4,5	70	1.29	3.16	1.34	3.00
5 scenes	1,2,3,4,5	74	1.62	3.88	1.68	3.62

It is noteworthy that accuracy to better than 0.5 pixels is achieved for correction Models A and PA for all single image orientations. The degradation when two images are merged is modest (except for the case where one of the images is the first in the strip), as it is in the orientation of the merged centre three images. For strip configurations comprising images at either end of the strip, i.e. two 3-image configuration and all 4- and 5-image cases, accuracy degrades but still remains sub-pixel in the cross-track direction, whereas it

* Review Paper – accepted after double-blind review.
ISBN: 978-0-9872527-1-5
Melbourne: Geospatial Sciences, RMIT 2012

falls off to reach 1.8 pixels in the flight direction. The accuracy degradation in the along-track direction for multi-image strips indicates that perturbations in the orbit and attitude of the THEOS platform cannot be fully compensated through offset correction parameters. This is contrary to the experience with strip adjustment of strips of tens of ALOS PRISM images (Fraser & Ravanbakhsh, 2010). Nevertheless, georeferencing to 2-pixel accuracy is quite sufficient for numerous remote sensing applications.

In Case 2, configurations of 6 GCPs (assigned standard error of 0.1m) were used for orientation adjustments of both single images and those combinations of images that did not include the first and last image from the strip. From this series of adjustments an estimate of planimetric georeferencing accuracy could be made based on the 2D residuals at ground checkpoints. Only one bias-correction model was used, the 3-parameter attitude correction Model A. The resulting planimetric checkpoint RMSE values are listed in Table 4.

Table 4. Planimetric georeferencing accuracy expressed via RMS discrepancies at ground checkpoints.

Number of merged scenes	Scene index	Number of Checkpoints	RMSE, Model A	
			Easting (m)	Northing (m)
1 scene	1	2	0.61	0.56
	2	7	0.58	0.57
	3	10	0.67	0.92
	4	26	0.73	0.88
	5	23	0.57	0.92
2 scenes	2,3	20	0.84	1.14
	3,4	36	1.40	1.51
3 scenes	2,3,4	46	1.44	1.71

It should be recalled that these arise from single configurations of 6 GCPs and variations in checkpoint discrepancy values can be expected with different control point configurations. The first feature of note in Table 4 is that sub-pixel accuracy is achieved in all cases, even in the multi-scene configurations, although accuracy in these instances is lower than that achieved for the relatively more controlled single images. Overall, while the RMSE values listed in Table 4 are larger than the corresponding internal accuracy measures in Table 3, they are basically consistent for all practical purposes. The accuracy attained in the along-track direction is a little worse than that in the cross-track direction for multi-image strips, which is also consistent with the internal accuracy achieved. This difference is likely the result of incomplete error compensation in the pitch angle observations.

5. CONCLUDING REMARKS

The georeferencing accuracy of a 5-scene strip of THEOS panchromatic mono imagery has been assessed through application of a generic pushbroom sensor orientation model for high-resolution satellite imagery. Application of this model, coupled with a modeling and correction of IO parameters derived from the THEOS metadata, have yielded sub-pixel (0.5-2m) 2D georeferencing accuracy in 3-image strip adjustments utilizing only six GCPs. The IO errors, introduced by what is suspected to be imprecise view angles in the metadata, can be modelled and corrected using cubic polynomials. As a result, *x*-image coordinate residuals could be reduced from 2 pixels RMS to sub-pixel level, leading to sub-pixel georeferencing accuracy. Through the orientation of multi-image strips via the strip adjustment approach, it was also possible to highlight that although a 3-parameter correction model for attitude biases was sufficient to yield sub-pixel accuracy in strip arrangements of three images, this was not the case for strip configurations involving the first and last image from the sequence of five. Whether this is due to perturbations in the THEOS platform

* Review Paper – accepted after double-blind review.
ISBN: 978-0-9872527-1-5
Melbourne: Geospatial Sciences, RMIT 2012

or is a consequence of having insufficient orbit observations at and beyond the extremities of the strip of images is still to be fully investigated.

6. ACKNOWLEDGEMENTS

The authors thank GISTDA for providing the THEOS imagery in this research.

7. REFERENCES

Chen, L.C. & Lee, L.-H., 1993. Rigorous generation of digital orthophotos from SPOT images. Photogrammetric Engineering and Remote Sensing, 59(5): 655-661.

Dowman, I. & Michalis, P., 2003. Generic rigorous model for along track stereo satellite sensors. Proceedings of Joint Workshop on High Resolution Mapping from Space (Eds. M. Schroeder, K. Jacobsen & C, Heipke), 6 – 8 October, Hanover, Germany. 6 pages on CD-ROM.

Fraser, C.S. & Hanley H.B., 2003. Bias compensation in rational functions for IKONOS satellite imagery. *Photogrammetric Engineering and Remote Sensing*, 69(1): 53-57.

Fraser, C.S., Rottensteiner, F., Weser, T. & Willneff, J., 2007. Application of a Generic Sensor Orientation Model to SPOT 5, QuickBird and ALOS Imagery. *Proceedings, 28th Asian Conference on Remote Sensing, ACRS 2007*, Kuala Lumpur, 12-16 Nov., 7 pages (on CD-ROM).

Fraser, C.S. & Ravanbakhsh, M., 2010. Precise Georeferencing of Long Strips of ALOS Imagery. *Photogrammetric Engineering & Remote Sensing*, 77(1): 87-93.

GISTDA, 2010. THEOS DIMAP/GeoTIFF Format and Description, Version 1.1.

Kim, T. & Dowman, I., 2006. Comparison of two physical sensor models for satellite images: Position-Rotation model and Orbit-Attitude model. *Photogrammetric Record*, 21(114): 110-123.

Kocaman, S. & Gruen, A. 2008. Geometric Modeling and Validation of ALOS/PRISM Imagery and Products. *International Archives of Photogrammetry, Remote Sensing and Spatial Information Sciences*, Beijing, China. Vol. XXXVI, Part 3: 12-18.

Kratky, V., 1989. Rigorous photogrammetric processing of SPOT images at CCM Canada. *ISPRS Journal of Photogrammetry and Remote Sensing*, 44(2): 53–71.

Michalis, P. & Dowman, I., 2008. A Generic Model for Along-track Stereo Sensors Using Rigorous Orbit Mechanics. *Photogrammetric Engineering & Remote Sensing*, 74(3): 303-309.

Poli, D., 2005. *Modelling of spaceborne linear array sensors*. Doctoral thesis, IGP Report No. 85, Institute of Geodesy and Photogrammetry, ETH Zurich, Switzerland. 204 pages.

Radhadevi, P. V., Müller, R., d'Angelo, P. and Reinartz, P. 2011. In-flight Geometric Calibration and Orientation of ALOS/PRISM Imagery with a Generic Sensor Model. *Photogrammetric Engineering and Remote Sensing*, 77(5): 531-538.

Rottensteiner, F., Weser, T., Lewis, A., & Fraser, C.S., 2009. A Strip Adjustment Approach for Precise Georeferencing of ALOS Imagery. *IEEE Trans. on Geoscience and Rem. Sens.*, 47(12): 4083-4091.

Weser, T., Rottensteiner, F., Willneff, J., Poon J. & Fraser C.S., 2008. Development and testing of a generic sensor model for pushbroom satellite imagery. *Photogrammetric Record*, 23(123): 255-274.

Westin, T., 1990. Precision rectification of SPOT imagery. *Photogrammetric Engineering and Remote Sensing*, 56(2): 247–253.

Xu, G., 2007. *Coordinate and Time Systems in GPS: Theory, Algorithms, and Applications, Chap. 2 (2nd Ed.).* Springer Berlin Heidelberg, New York, pp.7-20.

* Review Paper – accepted after double-blind review.
ISBN: 978-0-9872527-1-5